

**Instanton-dyon ensembles with quarks with modified boundary conditions**

Rasmus Larsen and Edward Shuryak

*Department of Physics and Astronomy, Stony Brook University, Stony Brook, New York 11794-3800, USA*

(Received 23 September 2016; published 11 November 2016)

We modify the quark periodicity condition on the thermal circle by the introduction of some phases—known also as “flavor holonomies”—different quark flavors. These phases provide a valuable tool, to be used for better understanding of deconfinement and chiral restoration phase transitions: by changing them, one can dramatically modify both phase transitions. In the language of instanton constituents—instanton-dyons or monopoles—changing the quark periodicity condition has a very direct explanation: the interplay of flavor and color holonomies can switch topological zero modes between various dyon types. The model we will study in detail, the so-called  $Z_{N_c}$ -symmetric QCD model with equal number of colors and flavors  $N_c = N_f = 2$  and special arrangement of flavor and color holonomies, ensures the “most democratic” setting, in which each quark flavor and each dyon type are in one-to-one correspondence. The usual QCD has the opposite “most exclusive” arrangement: all quarks are antiperiodic and, thus, all zero modes fall on only one—twisted or  $L$ —dyon type. As we show by ensemble simulation, deconfinement and chiral restoration phase transitions in these two models are dramatically different. In the usual QCD, both are smooth crossovers: but in the case of the  $Z_2$ -symmetric model, deconfinement becomes a strong first-order transition, while chiral symmetry remains broken for all dyon densities studied. These results are in good correspondence with those from recent lattice simulations.

DOI: [10.1103/PhysRevD.94.094009](https://doi.org/10.1103/PhysRevD.94.094009)**I. INTRODUCTION**

QCD-like gauge theories display two main nonperturbative phenomena—confinement and spontaneous breaking of  $SU(N_f)$  chiral symmetry. Their mechanism has been discussed extensively since the 1970s: we will mention some historical highlights below. Our previous papers, referred to as I [1] and II [2] below, address those phenomena in a model based on a certain gauge topology model.

Before going into the details of that model, let us first explain the main new element of this paper—what we mean by quark periodicity condition and why one should be interested in such theories. The standard Euclidean formulation of QCD-like theories define time  $\tau \in S^1$ , on the so-called Matsubara circle with a circumference  $\beta = \hbar/T$ . Bosons—the gauge fields—are periodic on this circle, and fermions are antiperiodic: as a result, standard Bose and Fermi thermal factors automatically appear in thermodynamical expressions. One can generalize quarks periodicity condition on  $S^1$  by adding an arbitrary phase, and this is the option used in this work. With a generic value of this phase, quarks are neither fermions nor bosons: perhaps one can use a term originated from condensed matter physics—the “anyons.”

The short answer to why such studies can be instructive follows: chiral symmetry breaking is associated with Dirac zero modes of certain topological solitons. By changing the quark phases, one can very effectively manipulate their coupling to solitons of different kinds and, thus, learn which of them are in fact relevant for the phenomena under consideration.

Since this is our third paper of the series, it hardly needs an extensive introduction. Here is a brief outline of the historic development of nonperturbative QCD. Since the 1970s, confinement was historically connected with gauge field solitons with magnetic charge—the monopoles. It is sufficient to mention the so-called “dual superconductor” model by ’t Hooft and Mandelstam [3] and Polyakov’s proof of confinement in  $2 + 1$ -dimensional gauge theories [4].

Chiral symmetry breaking was first addressed back in 1961 by Nambu and Jona Lasinio (NJL) [5], who pointed out the existence of the chiral symmetry, as well as its spontaneous breaking by a nonzero quark condensate. It was shown that in order to create it, some strong attractive 4-fermion interaction is needed, at momenta below a cutoff  $Q < \Lambda \sim 1$  GeV. Twenty years later, the emerging instanton phenomenology [6] made it clear that this interaction is nothing more than multifermion effective forces induced by instantons. Furthermore, unlike the effective Lagrangian conjectured by NJL, it also explicitly breaks  $U(1)_a$  axial symmetry. With time, a somewhat different perspective on chiral symmetry breaking developed, focused on the Dirac eigenvalue spectrum. The low-lying eigenvalues are formed via collectivization of the topological fermionic zero modes into the so-called zero mode zone (ZMZ); for a review, see [7].

While the main nonperturbative phenomena were for a long time ascribed to two rather distinct mechanisms, the results of the numerical simulations on the lattice persistently indicated that the deconfinement temperature  $T_{\text{deconf}}$

and chiral symmetry restoration, one to be called  $T_\chi$ , are in fact very close, at least for near-real-world QCD (with the number of colors and flavors  $N_c = 3$ ,  $N_f = 2 + 1$  and quark masses small). This fact, and in general their interplay in all QCD-like theories became one of the most puzzling issues in nonperturbative QFT.

But does it really hold for all QCD-like theories? One simple way to modify QCD is to change the color charge (representation) of the quark fields. Changing the quark color charge from the fundamental to adjoint representation, Kogut [8] observed in  $SU(2)$  gauge theories (with two and four species of Majorana fermions, or one and two species of the Dirac ones) two distinct phase transitions, at temperatures separated by a large factor:

$$\frac{T_\chi^{a\text{QCD}}}{T_{\text{deconf}}^{a\text{QCD}}} \sim O(10). \quad (1)$$

Later studies for the  $SU(3)$  theories with adjoint quarks [9,10] also observed such a large separation. Such a significant split between two transition temperatures may suggest that some quite different mechanisms are responsible for these two phenomena. Our studies of the adjoint quarks will be described in a separate publication, IV [11].

On the other hand, theory developments revealed some common dynamical roots of confinement and chiral symmetry breaking. In 1998, when the finite-temperature instantons were generalized to the case of the nonzero expectation value of the Polyakov loop by Lee-Li-Kraanvan Baal [12,13], it became apparent that each consists of  $N_c$  objects, known as instanton-dyons (or instanton-monopoles). Unlike instantons themselves, their constituents have charges and directly backreact on the holonomy value. This observation led to the proposal [14] of confinement being driven by this effect and, in a very specialized setting, it has been shown to induce confinement [15,16], even for exponentially small dyon density. Recent works using mean-field methods [17,18] and our own two papers [1,2] have shown that a sufficiently dense ensemble of the dyons does generate both confinement and chiral symmetry breaking, with close transition temperatures (too close to separate inside the errors).

Let us now turn to the discussion of quarks with nonstandard periodicity phases on  $S^1$ : can those have any measurable physical effect on observables? A first experimentation with quark phases [19] answered this question affirmatively. Even with fixed quenched lattice gauge configurations, it was confirmed that the value of the quark condensate depends on the periodicity phase. In particular, the “periodic” (or bosonic) quarks possess chiral symmetry breaking until very high  $T$ , in striking contrast to the usual antiperiodic ones. A suggested explanation [20] was formulated in terms of the instanton-dyons: the periodic quarks have zero modes with M-type dyons, while the antiperiodic quarks have zero modes with

“twisted” L-type dyons. The “masses” (actions) of those are different at  $T > T_{\text{conf}}$  and the twisted ones  $L$  are heavier  $S_L > S_M$  and, therefore, have smaller density:

$$n_M \gg n_L. \quad (2)$$

So, the periodic quarks “see” a much denser ( $M$  dyon) ensemble than the antiperiodic ones, which explains the larger quark condensate and higher  $T_\chi$ .

In a framework of the PNJL model, Kouno *et al.* [21–25] suggested to require different boundary conditions to different quark flavors. For enhanced symmetry, they focus on theories in which the number of colors and flavors are the same,  $N_c = N_f$ . In particular, for the  $SU(3)$  color, they use quark angles for  $u$ ,  $d$ ,  $s$  quarks to be of the form  $(0, \theta, -\theta)$ , respectively. The parameter  $\theta$  can be varied from  $\theta = 0$  (the usual QCD) to  $\theta = 2\pi/3$ , at which point the theory becomes “center symmetric.” Thus, the name of the resulting model— $Z_{N_c}$ -symmetric QCD. In the framework of the PNJL model, these authors found substantial dependence of  $T_\chi$  on  $\theta$ . The effect is the largest for the symmetric value:

$$T_\chi^{Z_3\text{QCD}} \approx 2T_{\text{deconf}}^{Z_3\text{QCD}}. \quad (3)$$

Of course, the PNJL is just a model, using as input the holonomy potential and the 4-quark NJL-like Lagrangian, the same as for ordinary QCD, with unmodified parameters: whether this can be justified is unclear.

The flavor-dependent phases were also suggested in the framework of supersymmetric QCD in [26].

Misumi *et al.* [27] recently put this  $Z_3$ -symmetric theory on the lattice. They observed that, compared to ordinary QCD, in this case the deconfinement transition is significantly strengthened to the first-order phase transition, with clear hysteresis, etc. The chiral breaking for the  $Z_3$ -symmetric theory is indeed present at higher temperatures. It is hard to tell from the paper, since small mass extrapolation is not yet performed, whether the chiral symmetry is in fact restored at any temperatures. Furthermore, the chiral condensates for different flavors become clearly different, so  $T_\chi$  should get split for different flavors. Qualitatively, the PNJL-based conclusions are confirmed.

## II. $Z_{N_c}$ -SYMMETRIC QCD AND THE INSTANTON-DYONS

Let us start this section by noting that, in the framework of the original instanton model, most of the phenomena mentioned in the Introduction would be impossible to explain. Indeed, the number of zero modes of the instanton is prescribed by the topological index theorem and is independent of the periodicity condition.

On the other hand, after it has been recognized that instantons have to be split into instanton-dyons, the

situation changes dramatically. Indeed, quarks with different boundary angles can be coupled to different types of dyons. Dialing different values of those angles, one can see the consequences from which it will eventually be possible to understand the dynamical role of those objects.

The “ $Z_{N_c}$ -symmetric QCD” proposed by Kouna *et al.* does indeed have outstandingly simple symmetry properties in the instanton-dyon model: each quark flavor has zero modes with a different type of instanton-dyon. This means that each quark flavor has its own “dyon plasma” with which it interacts. We note that, in this model, the number of colors and flavors must match,  $N_f = N_c$ , so the number of quark and dyon types match as well.

Furthermore, in the low  $T$ , near and below  $T_{\text{deconf}}$ , the holonomy values tend to the symmetric “confining” value, at which all types of the dyons obtain the same action. This fact indeed made the model  $Z_{N_c}$  symmetric.

In the opposite limit of high  $T$ , the holonomy moves to a trivial value, and the actions of different dyons become distinct. This implies that each quark flavor has its own “dyon plasma” with distinct densities, leading to flavor-dependent  $T_\chi$ .

One more qualitative idea is related to the values of  $z$  which are “intermediate” between the extremes discussed above. Those are values at which the zero modes jump from one kind of dyon to the next. This happens by “delocalization” of the zero mode, which means that, at such particular  $z$  values, the zero modes become long range. Since in this case the “hopping” matrix elements, describing quark-induced dyon-dyon interactions, get enhanced, one may also expect that the chiral condensate is effectively strengthened.

### III. THE SETTING OF THE SIMULATIONS

Let us remind the reader of the setting used in our first paper [1] with instanton-dyons. A certain number of them—64 or 128—are placed on the three-dimensional sphere. Its radius, thus, controls the density. The standard Metropolis algorithm is used to numerically simulate the distribution defined by classical and one-loop partition function. We studied the simplest non-Abelian theory with two colors  $N_c = 2$ , which has a single holonomy parameter  $\nu \in [0, 1]$ . Free energy is calculated and the adjustable parameters of the model—the value of the holonomy  $\nu$  and densities of  $M$ - and  $L$ -type dyons—are placed at its minimum.

In this paper, each dyon couples to a different flavor of quarks. The partition function is therefore  $Z_2$  symmetric, under  $\nu \leftrightarrow \bar{\nu} = 1 - \nu$  and  $M \leftrightarrow L$  replacement. A distinct symmetric phase has minimal free energy at the symmetric point  $\nu = 1/2$ , and equal number of  $L$ ,  $M$  dyons. An asymmetric phase has free energy with two minima, away from the center  $\nu = 1/2$ : by default, the spontaneous breaking of  $Z_2$  is assumed to happen to a smaller value of  $\nu$ , so that at high  $T$  it goes to zero.

Following paper II [2], we use the following parametrization of the overlap between zero modes,

$$T_{ij} = v_k c' \exp\left(-\sqrt{11.2 + (v_k r T/2)^2}\right), \quad (4)$$

where  $v_k$  is  $v = 2\pi\nu$  for  $M$  dyons, and  $v_k$  is  $\bar{v} = 2\pi\bar{\nu} = 2\pi(1 - \nu)$  for  $L$  dyons. The three constants in the model are the same as our previous paper:  $x_0 = 2$  for the dimensionless size of the core,  $\Lambda = 4$  for the overall constant, and  $-\log(c') = -2.6$  for the constant on  $T_{ij}$ .

The simulations have been done using the standard Metropolis algorithm. An update of all  $N = 64$  or  $128$  dyons corresponds to one cycle. Each run consists of 3000 cycles. Free energy is measured by a standard trick, involving integration over the interaction parameter from zero to one. The simulation was done on a  $S^3$  circle, and its volume is  $V = 2\pi^2 r^3$ : we use  $r$  in some places below.

The input “action parameter”  $S$  defines the instanton-dyon amplitude and literally corresponds to the sum of the  $L$  and  $M$  dyon actions in the semiclassical amplitude. In one-loop approximation, it is related to the temperature  $T$  by the asymptotic freedom relation:

$$S = \left(\frac{11N_c}{3} - \frac{2N_f}{3}\right) \log\left(\frac{T}{\Lambda_T}\right). \quad (5)$$

In I and II, we approximately related the constant  $\Lambda_T$  to the phase transition temperature  $T_c$ : we do not do it in this work because there is no single phase transition in the theory we study now.

The varied parameters of the model include (i) The holonomy  $\nu$  which is related to the Polyakov loop as  $P = \cos(\pi\nu)$ , (ii) the densities of  $M$  and  $L$  dyons  $n_M$ ,  $n_L$ , and (iii) after the free energy is found for each run, the values of these parameters, corresponding to the minima, are fitted and used.

Other parameters include (iv) the Debye mass, which is used to describe the falloff of the fields: its value is kept “self-consistent” by a procedure explained in I. Finally, we mention (v) the auxiliary interaction variable which is then integrated in order to obtain the free energy  $F$ .

The organization of the numerical sets was done as follows. An initial survey found the areas of interest, corresponding to the minima of the free energy and the most important variations in the results. Then the final set of simulations was performed: the parameters are summarized in Table I. In total, 1,170,000 individual runs were done for the final set of data and were used to make the plots.

The main part of the data analysis consists of finding the minima of the free energy and getting the Debye mass self-consistent. To do the former, we fit data sets for the free energy near its minima with a two-dimensional parabola,

TABLE I. The input parameters used for the final set of simulations. The step sizes given are some standard ones: yet some areas was given extra attentions. For example, around  $N_M = 4$ , the step size was 1.

	Min	Max	Step size
$\lambda$	0	0.1	1/90
$\lambda$	0.1	1.0	0.1
$\nu$	0.05	0.55	0.025
$r$	1.2	1.8	0.05
$N_M$	3	18	2
$M_d$	1	3.5	0.5
$S$	5	9.5	0.5

$$f = (v - v_0)M(v - v_0) + f_0, \quad (6)$$

which has six variables.  $v$  and  $v_0$  are two-dimensional vectors with  $v$  containing the variables holonomy  $\nu$  and radius  $r$  and  $v_0$ , describing the position of the minimum.  $M$  is a 2 times 2 matrix with  $M = M^T$  containing the coefficients for the fit.

The fit was done on free energy values of  $5^2 = 25$  points from a square, containing five points around the minimum. The six parameters from the fit are used as follows: (i)  $v_0$  and its uncertainties give the values of densities and holonomy at the minimum, plotted as results below and (ii) the diagonal component of  $M$  in the holonomy direction was converted into the value of the Debye mass  $M_d$ . An additional requirement of the procedure, to make the ensemble approximately self-consistent, is that the Debye mass from the fit should be within  $\pm 0.25$  of the used input Debye mass value.

To obtain the chiral properties—such as the Dirac eigenvalue distributions and its dependence on dyon number and volume—we only used the “dominant” configurations for each action  $S$ .

The results reported below compare new results, for  $Z_2$ -symmetric QCD explained above, to the “old” ones, from II, for  $N_c = N_f = 2$  QCD with antiperiodic fundamental quarks.

#### IV. THE HOLONOMY POTENTIAL AND CONFINEMENT

The free energy density obtained from the simulations is shown in Fig. 1 as a function of holonomy value, both for standard (lower plot) and  $Z_2$ -symmetric QCD (upper plot). At high density of the dyons, one finds a symmetric minimum for the  $Z_2$ -symmetric model. As the density decreases, one finds behavior very different from both that of the quenched case (no quarks) with two minima or in standard QCD with broken center symmetry.

While symmetry remains intact, with the decreasing density (larger  $S$ ), the minima of the potential become very flat and wide. (A slight appearance of the minima can be

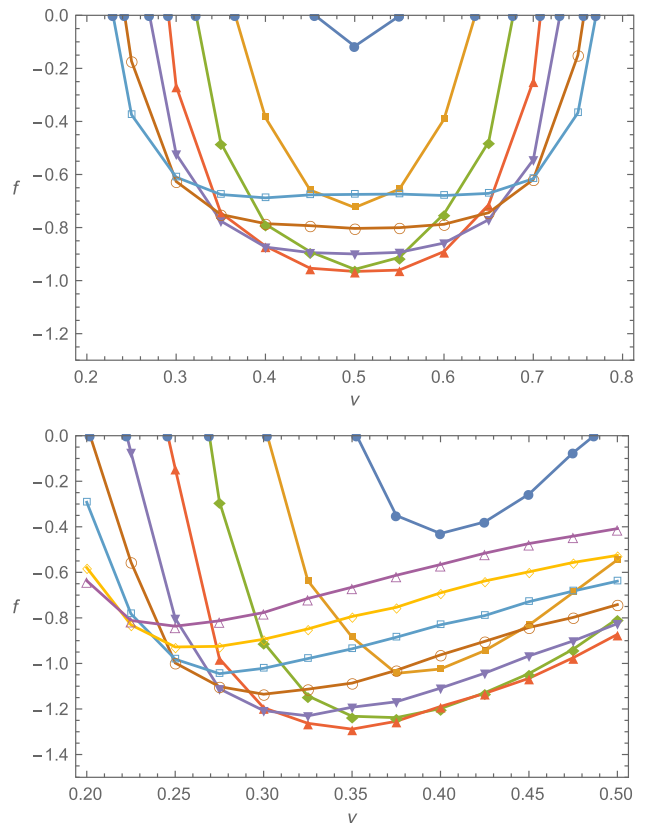


FIG. 1. Free-energy density as a function of the holonomy parameter  $\nu$ . The upper plot is for the  $Z_2$ -symmetric model and the lower plot is for the model in which all quarks are antiperiodic. Different curves are for different dyon densities. The densities are  $(0.47, \bullet)$ ,  $(0.37, \blacksquare)$ ,  $(0.30, \blacklozenge)$ ,  $(0.24, \blacktriangle)$ ,  $(0.20, \blacktriangledown)$ ,  $(0.16, \circ)$ ,  $(0.14, \square)$ ,  $(0.12, \diamond)$ ,  $(0.10, \triangle)$ . Not all densities are shown. In both cases, the action parameter is  $S = 8.5$  and both dyon types are equally represented  $n_M = n_L$ . Note the dramatic difference of the holonomy potentials for these two cases: the  $Z_2$  potential is symmetric (for equal dyon densities), while the periodic quarks produce an asymmetric minimum and thus slide smoothly towards smaller holonomies (to the left) as the dyon density decreases.

seen for the smallest density which is not nearly as strong as in the quenched case.) We interpret this as an appearance of a large domain of “mixed phase,” a coexistence of many different configurations with different properties and different  $\nu$ , but with degenerate free energy. The confining minimum in the middle is also found to be dominant for a much larger range of densities.

Translating the location of the minimum to the mean Polyakov line, we plot the results in Fig. 2. It shows that while the two models under consideration have very similar behavior at high densities of the dyons (smaller  $S$  or the left side of the plot), in the  $Z_2$ -symmetric model, there appears a strong jump in  $P$ , from about 0.2 to 0.6. Note that the intermediate point with the large error bar should be interpreted not as an uncertainty of the value, as the usual



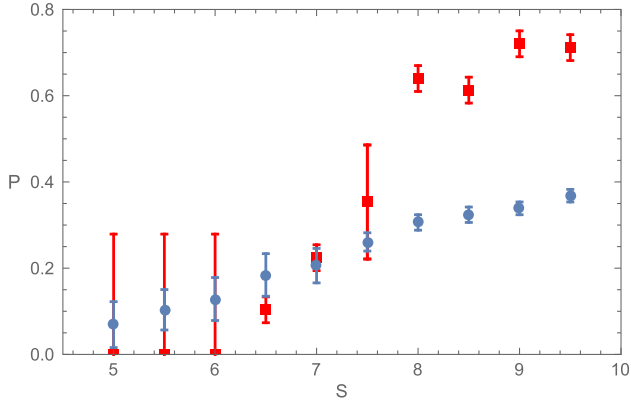


FIG. 2. The mean Polyakov loop  $P$  as a function of action parameter  $S$ , for the  $Z_2$ -symmetric model (red squares), compared to that for the  $N_c = N_f = 2$  QCD with the usual antiperiodic quarks (blue circles).

error bar, but rather as a reflection of the fact that, in the ensemble, the intermediate values of  $P$  are all feasible, due to flatness of the holonomy potential. In other words, this point is rather a vertical part of the curve, indicative of a strong first-order transition. This conclusion is consistent

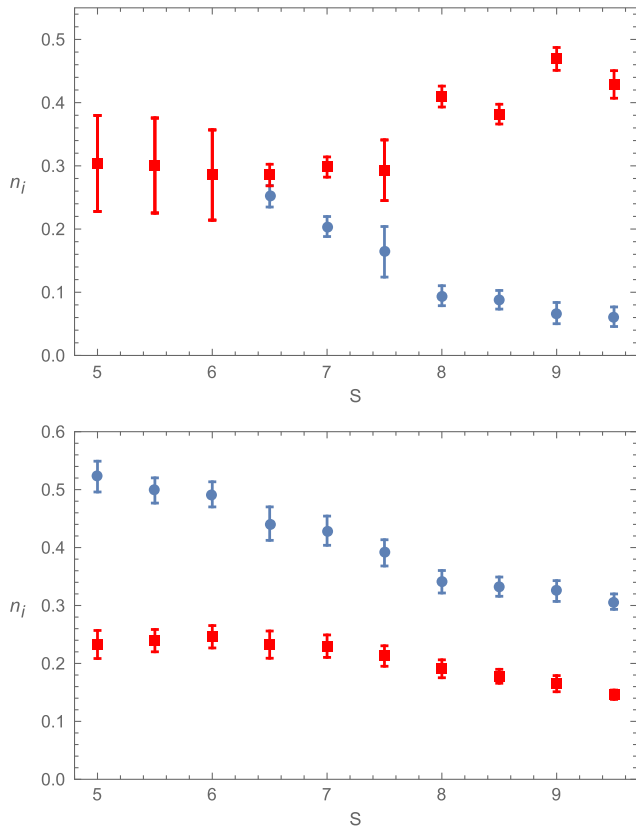


FIG. 3. (upper) Densities of  $L$  dyons (red squares) and  $M$  dyons (blue circles), as a function of action parameter  $S$ , for the  $Z_2$ -symmetric model. (lower) The same for the usual QCD-like model with  $N_c = N_f = 2$  and antiperiodic quarks.

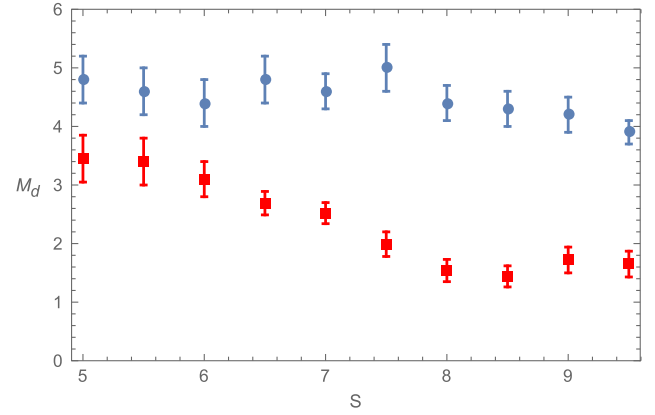


FIG. 4. Debye Mass  $M_d$  as a function of action parameter  $S$ , for the  $Z_2$ -symmetric model (red squares) and the usual QCD-like model with  $N_c = N_f = 2$  (blue circles).

with lattice studies in [27], in which the authors show some hysteresis curve for  $P$ , with a similar strong jump.

The densities of the dyons in both models are shown in Fig. 3. The upper plot for the  $Z_2$ -symmetric model displays a very symmetric confining phase at the lhs of the plot (small  $S$ , dense ensembles) complemented by a very asymmetric composition of the ensemble at the rhs. The usual QCD-like model with  $N_c = N_f = 2$  in the plot below shows that the  $L - M$  symmetry never holds, due to only  $L$ -dyons coupling to the zeromodes, while the overall dependence on  $S$  is much less significant.

Finally, the Debye mass—defined via the second derivatives of the effective potential at the minimum—has been determined and plotted in Fig. 4, again for both models. For the  $Z_2$ -symmetric model, its values are significantly lower than for the QCD-like model. Smaller mass indicates flatter potential and stronger fluctuations, already discussed above.

## V. CHIRAL SYMMETRY BREAKING

As we already explained above, the main feature of the  $Z_{N_c}$ -symmetric model with  $N_f = N_c$ , is that it distributes all types of quarks evenly, so that each type of dyon would have one quark flavor possessing zero modes. This is in contrast to the usual QCD, in which all quarks are antiperiodic and, thus, all have zero modes only with twisted  $L$ -type dyons.

The simplest examples considered in this work are two  $N_c = N_f = 2$  theories—the  $Z_2$ -symmetric model and the two color QCD. In the former case, the partition function includes two independent fermionic determinants, one for  $M$  and one for  $L$  dyons, with a single quark species each. In the latter, one has a square (two-species) of the determinant of the hopping matrix over the  $L$  dyons only.

Here we remind the reader of well-known facts about chiral symmetry breaking in such cases and the consequences for such determinants. Theories with a single

quark flavor have only a single  $U_a(1)$  symmetry, broken explicitly by the fermionic effective action. Indeed, it includes terms  $\bar{\psi}_L\psi_R$  or  $\bar{\psi}_R\psi_L$  directly coupling components with opposite chiralities. So, there are no chiral symmetries to break, and condensates are always nonzero, proportional to density of the topological objects.

The case with two or more flavors is different: there is the  $SU(N_f)$  flavor symmetry, which can be either broken or not, depending on the strength of the  $2N_f$ -quark effective interaction.

### A. Dirac eigenvalue distribution

Differences in chiral breaking mechanisms in these two models, indicated above, also manifest themselves in the Dirac eigenvalue distribution.

For a proper perspective, let us note that, for the  $SU(N_f)$  flavors with  $N_f \geq 2$ , a general Stern-Smilga theorem [28] states that the eigenvalue distribution at small  $\lambda$  has the so-called ‘‘cusp’’ singularity:

$$\rho(\lambda) = \frac{\Sigma}{\pi} \left( 1 + \frac{|\lambda|\Sigma(N_f^2 - 4)}{32\pi N_f F_c^4} + \dots \right). \quad (7)$$

For  $N_f > 2$ , the coefficient is positive—this is known as ‘‘direct cusp’’—and was also observed, both on the lattice and in the instanton models. In the particular case  $N_f = 2$ , this cusp is absent: this fact can be traced to the absence of the symmetric  $d^{abc}$  structure constant in the case of the  $SU(2)$  group. Indeed, both the calculations done in the instanton liquid framework (for examples and references see [7]) and our previous studies II of the  $N_f = 2$  theory had produced a ‘‘flat’’ eigenvalue distribution:

$$\rho_{N_f=2}(\lambda) \sim \text{const.} \quad (8)$$

In the  $N_f = 1$  case, the distribution does have a singularity at  $\lambda = 0$  of the form of the ‘‘inverse cusp’’,  $\sim -|\lambda|$ , with a negative coefficient. The Stern-Smilga derivation does not apply, but the theorem has been rederived for general  $N_f$  using partially quenched chiral perturbation theory in [29].

Our results for the  $Z_{N_c}$ -QCD under consideration shown in Fig. 5 also show the ‘‘inverse cusp’’ with linear behavior of  $\rho(\lambda)$ . (We use this fact to extrapolate  $\rho(\lambda)$  to  $\lambda \rightarrow 0$  and to extract the value of the quark condensate and the value of the coupling constant  $F_c$ .) In the other model,  $N_c = N_f = 2$  QCD, such an ‘‘inverse cusp’’ is absent; see II.

So far, our discussion has assumed an infinite volume limit in which case the Dirac eigenvalue spectrum extends until  $\lambda = 0$ . However, it is well known that any finite-size system, with 4-volume  $V_4$ , has the smallest eigenvalues of the order  $O(1/V_4)$ . This creates the so-called ‘‘finite size dip,’’ in the eigenvalue distribution, also clearly visible in Fig. 5 (upper). One can see that doubling of the volume,

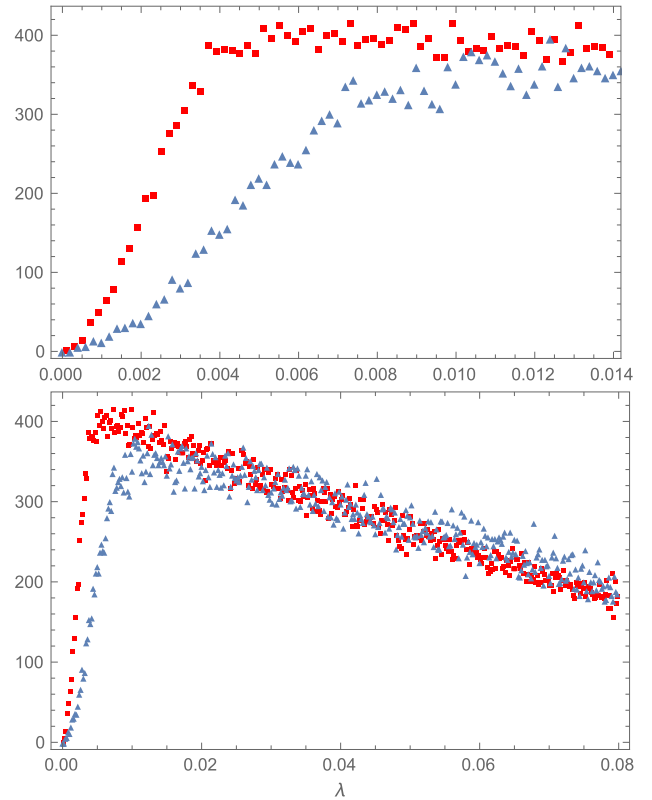


FIG. 5. The Dirac eigenvalue distribution  $\rho(\lambda)$  for ensembles of 64 (Blue triangle) and 128 (Red square) dyons, for  $Z_2$ -symmetric model at  $S = 6$ . The upper plot shows the region of smaller eigenvalues, in which one can see the finite volume ‘‘dip,’’ of a width which scales approximately as  $1/V_4$  as expected. The lower plot shows the same data sets, but in a wider range of eigenvalues: it displays the ‘‘inverse cusp’’ shape of the distribution discussed in the text.

from 64 to 128 dyons at the same density, reduces the width of this dip roughly by a factor of 2, as expected.

As the holonomy jumps away from its confining value 0.5, the dyon densities become different. Unlike the fundamental quarks, where the holonomy goes down, the densities of  $L$  dyons become larger than those of  $M$  dyons. The total density goes down, but the reduction in  $M$  dyons leaves space for a few more  $L$  dyons. This means that, on one hand, the density is larger for  $L$  dyons, and the zero-mode density is therefore higher. On the other hand, the factor in the exponential in  $T_{ij}$  [Eq. (4)] is  $\bar{\nu} = 1 - \nu$  for  $L$  dyons and  $\nu$  for  $M$  dyons. This means that, as  $\nu$  becomes smaller, the effective density of the zero modes associated with  $L$  dyons becomes smaller, while the zero modes associated with  $M$  dyons get an increased effective density. It is, therefore, the interplay between these two effects that control which of the condensates are largest. This results in what we show in Fig. 6, where the  $M$  dyon condensate appears to be slightly larger than the  $L$  dyon condensate, and both condensates decrease slightly in accordance with the total density of dyons. It is also observed that each gas

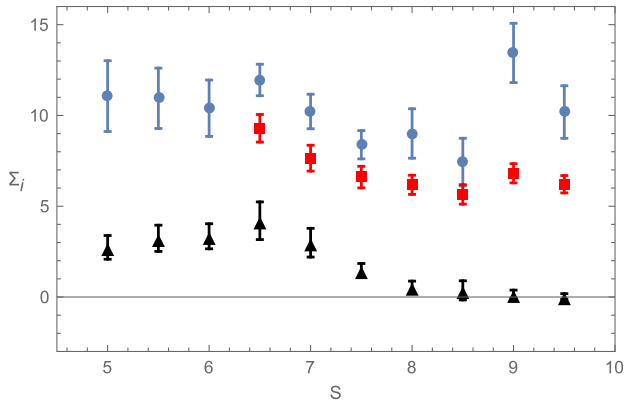


FIG. 6. Chiral condensate generated by  $u$  quarks and  $L$  dyons (red squares) and  $d$  quarks interacting with  $M$  dyons (blue circles) as a function of action  $S$ , for the  $Z_2$ -symmetric model. For comparison, we also show the results from II for the usual QCD-like model with  $N_c = N_f = 2$  by black triangles.

of zero modes effectively works as a  $N_f = 1$  ensemble, with nonvanishing condensates even at the lowest densities we studied [30] (the rhs of the plot). The other model— $N_c = N_f = 2$  QCD—has a condensate shown by black triangles: it clearly has chiral symmetry restoration: At  $S > 8$ , we detected no presence of a condensate.

The coupling constant  $F_c$  (Fig. 7), obtained from the slope of the eigenvalue distribution and Smilga-Stern theorem (7), is nearly density independent: it changes by a factor of around 1.5 from  $S = 5$  to  $S = 9.5$ . This is consistent with the behavior of the quark condensates and, similarly, indicates that, in the  $Z_2$  model, the chiral symmetry does not show a tendency to be restored.

## VI. SUMMARY AND DISCUSSION

To put it in perspective, let us start by briefly reminding the main findings of the previous two papers of these series. In I we had shown that in pure gauge theory with  $SU(2)$  color the instanton-dyon ensemble undergoes confinement transition as the dyon density reaches certain critical value. The high-density confining phase has holonomy  $\nu = 1/2$  and equal densities and other properties of all types of instanton-dyons.

In paper II, we added two light fundamental antiperiodic quarks, as they are in the  $SU(2)_c, SU(2)_f$  QCD. Deconfinement transition gets significantly smoothed to a crossover. Chiral symmetry transition is also somewhat smooth, and happens when the Polyakov loop gets close to the confining value  $P = 0$ . Thus, we concluded that the old question of the interrelation of the two transitions is finally over: a large enough instanton-dyon density does both.

In this work, we introduce flavor holonomies, and, following Kouno *et al.* [21], arrange them into the

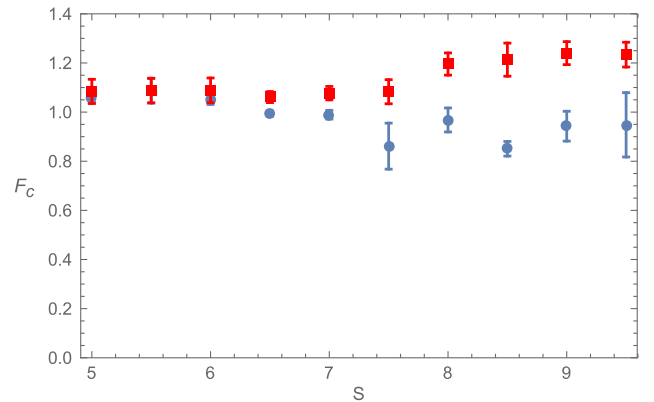


FIG. 7. Coupling constant  $F_c$  for the  $M$  dyon ensemble (blue circle) and the  $L$  dyon ensemble (red square).

$Z_2$ -symmetric model, which we compare to theories with all periodic or all antiperiodic (QCD) quarks. The results are dramatically different: the  $Z_2$ -symmetric model has very symmetric confining phase and a quick deconfinement transition, but no apparent chiral symmetry restoration. The deconfinement becomes much stronger, a first-order transition with clear mixed phase for intermediate dyon densities. Chiral symmetry seems to never be restored, even for the smallest densities, as indeed is expected based on analogy to the one-flavor QCD. Different flavors do have different condensates, but the difference in condensates is much smaller than the difference in the dyon densities. Our approach, based on instanton-dyons, provides the simplest explanation of these observations. The flavor-dependent periodicity condition effectively manipulate the coupling to dyons of different kinds. The  $Z_N$ -symmetric model is the “most democratic” arrangement, producing basically  $N$  copies of single-flavor topological ensembles, drastically different from one  $N$ -flavor ensemble of  $L$ -dyons in the usual QCD.

Thus, we take lattice confirmation of these phenomena, by Misumi *et al.* [27], as basically a confirmation of its main statement: chiral symmetry breaking is induced by zero modes of the instanton-dyons. Needless to say, more detailed studies on the lattice are possible: perhaps direct identification of the quasizero mode localization with the instanton-dyons in the gauge field ensemble would soon be possible.

## ACKNOWLEDGMENTS

We would like to thank T. Iritani and I. Zahed for useful discussions. This work was supported in part by the U.S. Department of Energy, Office of Science, under Contract No. DE-FG-88ER40388.

- [1] R. Larsen and E. Shuryak, Interacting ensemble of the instanton-dyons and the deconfinement phase transition in the SU(2) gauge theory, *Phys. Rev. D* **92**, 094022 (2015).
- [2] R. Larsen and E. Shuryak, Instanton-dyon ensemble with two dynamical quarks: The chiral symmetry breaking, *Phys. Rev. D* **93**, 054029 (2016).
- [3] Y. Nambu, Strings, monopoles, and gauge fields, *Phys. Rev. D* **10**, 4262 (1974); S. Mandelstam, II. Vortices and quark confinement in non-Abelian gauge theories, *Phys. Rep.* **23**, 245 (1976).
- [4] A. M. Polyakov, Quark confinement and topology of gauge groups, *Nucl. Phys.* **B120**, 429 (1977).
- [5] Y. Nambu, Axial Vector Current Conservation in Weak Interactions, *Phys. Rev. Lett.* **4**, 380 (1960); Quasi-particles and gauge invariance in the theory of superconductivity, *Phys. Rev.* **117**, 648 (1960); Y. Nambu and G. Jona-Lasinio, Dynamical model of elementary particles based on an analogy with superconductivity. I, *Phys. Rev.* **122**, 345 (1961).
- [6] E. V. Shuryak, The role of instantons in quantum chromodynamics. I. Physical vacuum, *Nucl. Phys.* **B203**, 93 (1982).
- [7] T. Schafer and E. V. Shuryak, Instantons in QCD, *Rev. Mod. Phys.* **70**, 323 (1998).
- [8] J. B. Kogut, Simulating simple supersymmetric field theories, *Phys. Lett. B* **187**, 347 (1987).
- [9] F. Karsch and M. Lutgemeier, Deconfinement and chiral symmetry restoration in an SU(3) gauge theory with adjoint fermions, *Nucl. Phys.* **B550**, 449 (1999).
- [10] G. Cossu, M. D’Elia, A. Di Giacomo, G. Lacagnina, and C. Pica, Monopole condensation in two-flavor adjoint QCD, *Phys. Rev. D* **77**, 074506 (2008).
- [11] R. Larsen and E. Shuryak, Instanton-dyon ensembles IV: Adjoint fermions (to be published).
- [12] T. C. Kraan and P. van Baal, Monopole constituents inside SU(n) calorons, *Phys. Lett. B* **435**, 389 (1998).
- [13] K.-M. Lee and C.-h. Lu, SU(2) calorons and magnetic monopoles, *Phys. Rev. D* **58**, 025011 (1998).
- [14] D. Diakonov, Topology and Confinement, *Nucl. Phys. B, Proc. Suppl.* **195**, 5 (2009); D. Diakonov and V. Petrov, Confining ensemble of dyons, *Phys. Rev. D* **76**, 056001 (2007).
- [15] E. Poppitz, T. Schaefer, and M. Unsal, Continuity, deconfinement, and (super) Yang-Mills theory, *J. High Energy Phys.* **10** (2012) 115.
- [16] E. Poppitz and M. Unsal, Seiberg-Witten and ‘Polyakov-like’ magnetic bion confinements are continuously connected, *J. High Energy Phys.* **07** (2011) 082.
- [17] Y. Liu, E. Shuryak, and I. Zahed, Confining dyon-antidyon Coulomb liquid model. I, *Phys. Rev. D* **92**, 085006 (2015).
- [18] Y. Liu, E. Shuryak, and I. Zahed, Light quarks in the screened dyon-antidyon Coulomb liquid model. II, *Phys. Rev. D* **92**, 085007 (2015).
- [19] C. Gattringer, M. Gockeler, P. E. L. Rakow, A. Schafer, W. Soldner, and T. Wettig, Lattice QCD at finite temperature: Evidence for calorons from the eigenvectors of the Dirac operator, *Nucl. Phys. B, Proc. Suppl.* **106–107**, 492 (2002).
- [20] E. Shuryak and T. Sulejmanpasic, The chiral symmetry breaking/restoration in dyonic vacuum, *Phys. Rev. D* **86**, 036001 (2012).
- [21] H. Kouno, Y. Sakai, T. Makiyama, K. Tokunaga, T. Sasaki, and M. Yahiro, Quark–gluon thermodynamics with the  $Z_{N_c}$  symmetry, *J. Phys. G* **39**, 085010 (2012).
- [22] Y. Sakai, H. Kouno, T. Sasaki, and M. Yahiro, The quarkyonic phase and the  $Z_{N_c}$  symmetry, *Phys. Lett. B* **718**, 130 (2012).
- [23] H. Kouno, T. Makiyama, T. Sasaki, Y. Sakai, and M. Yahiro, Confinement and  $Z_{N_c}$  symmetry in three-flavor QCD, *J. Phys. G* **40**, 095003 (2013).
- [24] H. Kouno, T. Misumi, K. Kashiwa, T. Makiyama, T. Sasaki, and M. Yahiro, Differences and similarities between fundamental and adjoint matters in SU(N) gauge theories, *Phys. Rev. D* **88**, 016002 (2013).
- [25] H. Kouno, K. Kashiwa, J. Takahashi, T. Misumi, and M. Yahiro, Understanding QCD at high density from a  $Z_3$ -symmetric QCD-like theory, *Phys. Rev. D* **93**, 056009 (2016).
- [26] E. Poppitz and T. Sulejmanpasic, (S)QCD on  $\mathbb{R}^3 \times \mathbb{S}^1$ : Screening of Polyakov loop by fundamental quarks and the demise of semi-classics, *J. High Energy Phys.* **09** (2013) 128.
- [27] T. Iritani, E. Itou, and T. Misumi, Lattice study on QCD-like theory with exact center symmetry, *J. High Energy Phys.* **11** (2015) 159.
- [28] A. V. Smilga and J. Stern, On the spectral density of Euclidean Dirac operator in QCD, *Phys. Lett. B* **318**, 531 (1993).
- [29] J. C. Osborn, D. Toublan, and J. J. M. Verbaarschot, From chiral random matrix theory to chiral perturbation theory, *Nucl. Phys.* **B540**, 317 (1999).
- [30] It should be noted that the chiral condensate is harder to study as the amount of dyons in the simulation becomes small, which happens for  $M$  dyons when there is a large asymmetry in the density. This explains larger error bars for one of the condensates and why we stopped our studies at those particular parameters.